Application Note
TMCS110x Layout Challenges and Best Practices

Carolus Andrews, Patrick Simmons   *Current Sensing*

ABSTRACT

Hall-based current sensors provide multiple benefits that are not typically found in current shunt monitors. These benefits include isolation, as well as the ability to operate inside of high working voltage and AC environments. While providing such benefits, designing with Hall-based devices presents a system designer with a different set of challenges. This application report delves into some of the challenges pertaining to Hall-based current monitors, including output limitations, limitations on current measurement, layout challenges, and contributions from external fields. It then provides insights on how to mitigate these environmental and layout related sources of error.

Table of Contents

Trademarks

All trademarks are the property of their respective owners.

1 Introduction

This application note begins with a discussion of device operation and device specifications. The document continues with best practices for the TMCS110x product family, including grounding techniques, output stage limitations, as well as various sources of external fields and how to combat them.

2 Device Operation

To better comprehend what affects measurement errors with a Hall-based current sensor like the TMCS1100, understanding how the device operates in a general sense is helpful. TMCS1100 Operation Diagram illustrates how current flows through the copper lead frame of the device. As the current flows from IN+ to IN−, a magnetic field is generated in accordance with Ampere's law. This magnetic field produces a voltage potential change on sensors located in the center of the lead frame via the Hall-effect . This potential is then scaled, sampled by the sampling integrator, and sent to the output pin of the device. Note that the positive polarity of the magnetic coupling factor as current flows from IN+ to IN− is a magnetic field generated downward into the sensor, denoted in this paper as the negative z direction.

For any given TMCS110x device, there are typically multiple sensitivity variants. For the TMCS1100, the sensitivities include 50 mV/A, 100 mV/A, 200 mV/A, and 400 mV/A. For each device, the lead frame and the Hall stage are the same for all variants within some manufacturing tolerance.
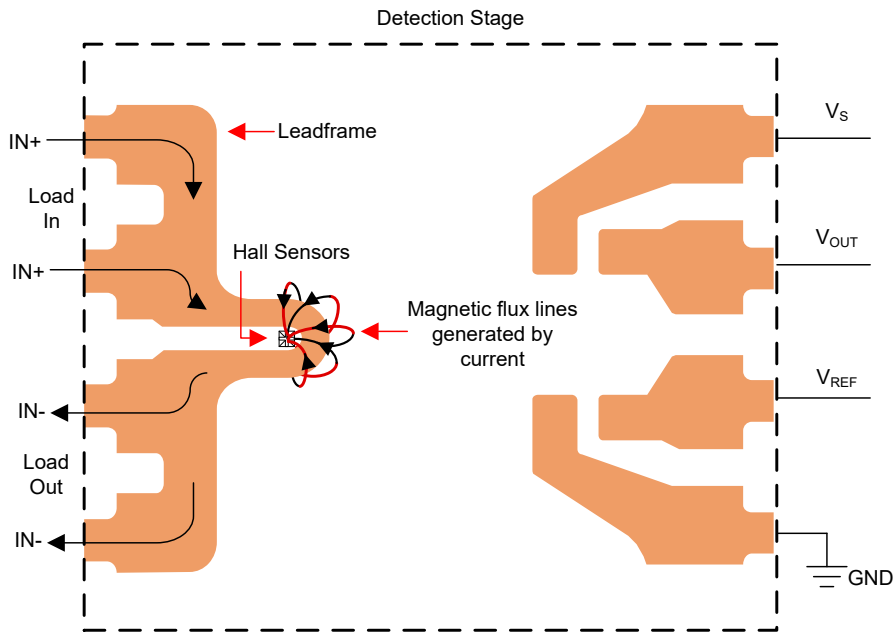
Figure 2-1. TMCS1100 Operation Diagram

3 Grounding

A key feature of the TMCS110x device family is temperature compensation. This allows a given TMCS110x device to achieve a low-sensitivity drift of ±0.5% over temperature and lifetime. This compensation is achieved through internal circuitry that utilizes a clock, which contains pulsing components, and therefore requires a properly-designed ground path. While a low-resistance path between device ground and the central system ground is a good practice in general, the digital clock provides a dynamic current component that can further influence measurement precision. Therefore, Equation 1 is used to approximate what kind of offset might be observed for a given device ground to system ground return path, where the values of resistance and inductance are quantifiable from the planes or traces between the GND pin of the TMCS1100 and the system ground.

$$V_{GNDOFFSET} = I_Q R_{trace} + L_{trace}\frac{di_q}{dt} \tag{1}$$

As the path to system ground becomes more complex, the effect of these artifacts becomes more apparent as added offset and noise on the output of the device. To demonstrate this, a long, discrete coiled wire was used in place of the ground plane on a TMCS1100EVM to emulate a long trace between the GND pin and system GND of the module. In addition, the bypass capacitor was also removed from the EVM to provide a worst-case look at the effects of these artifacts on the device. TMCS1100EVM With "Poor" Inductive Ground Path shows the output of the A2 device variant in this state, with no input current supplied to the device.
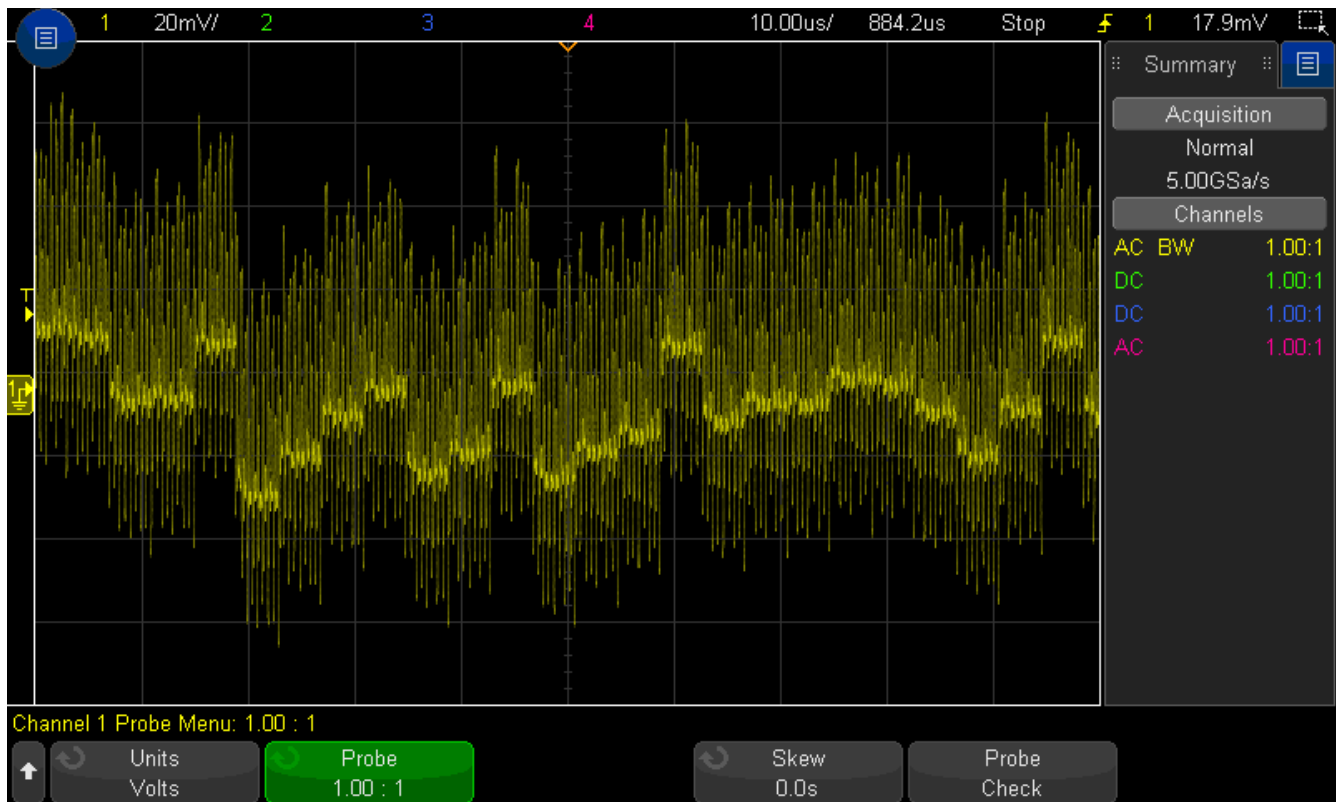
Figure 3-1. TMCS1100EVM With "Poor" Inductive Ground Path

An ideal grounding path is a direct path from the GND pin of the device to the system GND of the board, using as wide of a trace as possible to minimize resistance and inductance between the connection points. A GND plane as used on the TMCS1100EVM is ideal. TMCS1100EVM Default "Good" Ground Path shows the output of the A1 variant under ideal grounding conditions.
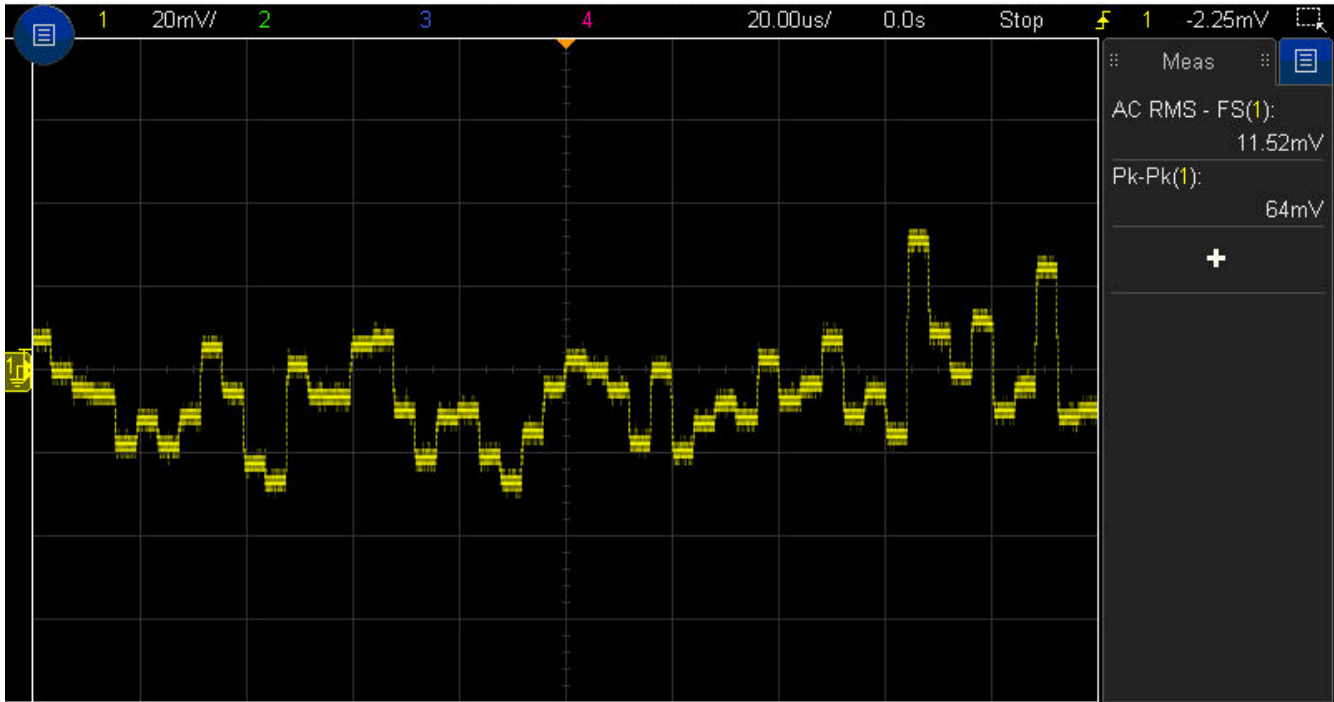
Figure 3-2. TMCS1100EVM Default "Good" Ground Path

Note that the "good" ground of the device still retains bouncing artifacts. This is expected as systematic noise comes from the sampling integrator used to compensate for temperature and lifetime drift, and is discussed in depth in the next section. In most designs, a wide ground plane as mentioned is not always achievable, but consideration must be given to how the device GND pin interfaces with the true ground of the system for best performance.

4 Measurement Range

4.1 Swing Limitations

Neglecting the influences of external error sources, which varies from design and operating environment, it is important to note that there are two bounds of output to examine for the device: the swing limit, and the linear operating range.

The first boundaries to consider are the swing limitations of the device. TMCS1101 Data Sheet: Swing Specifications shows the swing limitations, and demonstrates the maximum voltages that can actually be output by the device before entering a saturated condition. These bounds of output voltage for each sensing direction are determined from Equation 2 and Equation 3. The results of these equations give the range that the device is capable of measuring for the chosen operating conditions of V_{REF} and V_s.

$$I_{Forward} \leq \frac{Swing\_to\_V_S, max - V_{REF}}{Sensitivity} \tag{2}$$

$$I_{Reverse} \geq \frac{Swing\_to\_GND, max - V_{REF}}{Sensitivity} \tag{3}$$

Table 4-1. TMCS1101 Data Sheet: Swing Specifications

PARAMETERS		TEST CONDITIONS	MIN	TYP	MAX	UNIT
VOLTAGE OUTPUT						
	Swing to V_S power-supply rail	R_L = 10 kΩ to GND, T_A= –40°C to +125°C		V_S – 0.02	V_S – 0.1	V
	Swing to GND, current driven	R_L = 10 kΩ to GND, T_A= –40°C to +125°C		V_{GND} + 5	V_{GND} + 10	mV

The second boundary, which is a smaller subset located within the swing conditions, is the linear operating range, given for each device in TMCS1101 Data Sheet: Linear Operating Region.

Table 4-2. TMCS1101 Data Sheet: Linear Operating Region

PRODUCT	SENSITIVITY	ZERO CURRENT OUTPUT VOLTAGE,	I_{IN} LINEAR MEASUREMENT RANGE	
	$\Delta V_{OUT} / \Delta I_{IN+, IN–}$	$V_{OUT,0A}$	V_S = 5 V	V_S = 3.3 V
TMCS1101A1B-Q1	50 mV/A		±46 A	±29 A
TMCS1101A2B-Q1	100 mV/A		±23 A	±14.5 A
TMCS1101A3B-Q1	200 mV/A	0.5 × V_S	±11.5 A	±7.25 A
TMCS1101A4B-Q1	400 mV/A		±5.75 A	–
TMCS1101A1U-Q1	50 mV/A		–9 A → 86 A	–5.6 A → 55.4 A
TMCS1101A2U-Q1	100 mV/A		–4.5 A → 43A	–2.8 A → 27.7 A
TMCS1101A3U-Q1	200 mV/A	0.1 × V_S	–2.25 A → 21.5 A	–1.4 A → 13.85 A
TMCS1101A4U-Q1	400 mV/A		–1.12 A → 10.75 A	–

This smaller subset is the range to which the sensitivity error of the device has been applied, and is ensured to operate within the data sheet specification. Care must also be taken to ensure that current levels remain below both allowable continuous DC/RMS and transient peak current safe operating areas to not exceed device thermal limits. More information on this can be found in the Safe Operating Area section of the data sheet. In short, this shows that while the TMCS1101 may be configured to work to the voltage outputs of the swing limitation, the linearity may be slightly worse at the areas of output that fall outside the linear operating range. For optimal performance, ensure that the design is kept to within the linear operating region.

See the *Under the Hood: Output Swing Limitations of Current Sense Amplifiers* application report for reasons behind these limitations.

4.2 Noise Limitations

In the absence of an input current signal, the output noise is very dependent on grounding techniques as discussed in the Grounding section. Even with proper grounding techniques, a systematic noise remains due to the sampling integrator used to minimize temperature and lifetime drift. The input is sampled every 4 µs and the output is updated at a 250-kHz update rate, as discussed in the data sheet. In many cases, the impact of this noise floor can be minimized with a simple low-pass filter on the output of the device. However, first consider the RMS and peak-to-peak output noise from the device. To begin, the RMS and peak-to-peak noise output of the device under consideration can be determined using Equation 4 and Equation 5. The referred-to-input (RTI) noise density specifications are listed from the data sheet in TMCS1101 Data Sheet: Noise Density, RTI for convenience.

$$\text{Output Noise}_{RMS} = \text{Noise Density} \left(\mu A / \sqrt{Hz}\right) \times \sqrt{\text{Device Bandwidth}} \times \text{Sensitivity}(V/A) \tag{4}$$

$$\text{Output Noise}_{pk-pk} = \text{Output Noise}_{RMS} \times 6.6 \tag{5}$$

Table 4-3. TMCS1101 Data Sheet: Noise Density, RTI

PARAMETERS		TEST CONDITIONS	MIN	TYP	MAX	UNIT
OUTPUT						
Noise density, RTI		TMCS1100A1		380		µA/√ Hz
		TMCS1100A2		330		µA/√ Hz
		TMCS1100A3		300		µA/√ Hz
		TMCS1100A4		225		µA/√ Hz

These equations provide the theoretical RMS and peak-to-peak noise levels of each device, with the peak-to-peak calculation accounting for 99.9% of the distribution of the spectrum in the peak-to-peak measurement (for more information on how to calculate noise, see the our Analog Engineer's Pocket Reference). Figure 4-1 through Figure 4-4 show the noise floor of each TMCS1100 gain variants captured on the TMCS1100EVM with no output filtering. It can be observed that, as expected, the noise floor grows in proportion with the sensitivity, shown in the previous noise equations. Note that the RMS and peak-to-peak noise floor values are shown on the scope for each plot as well.
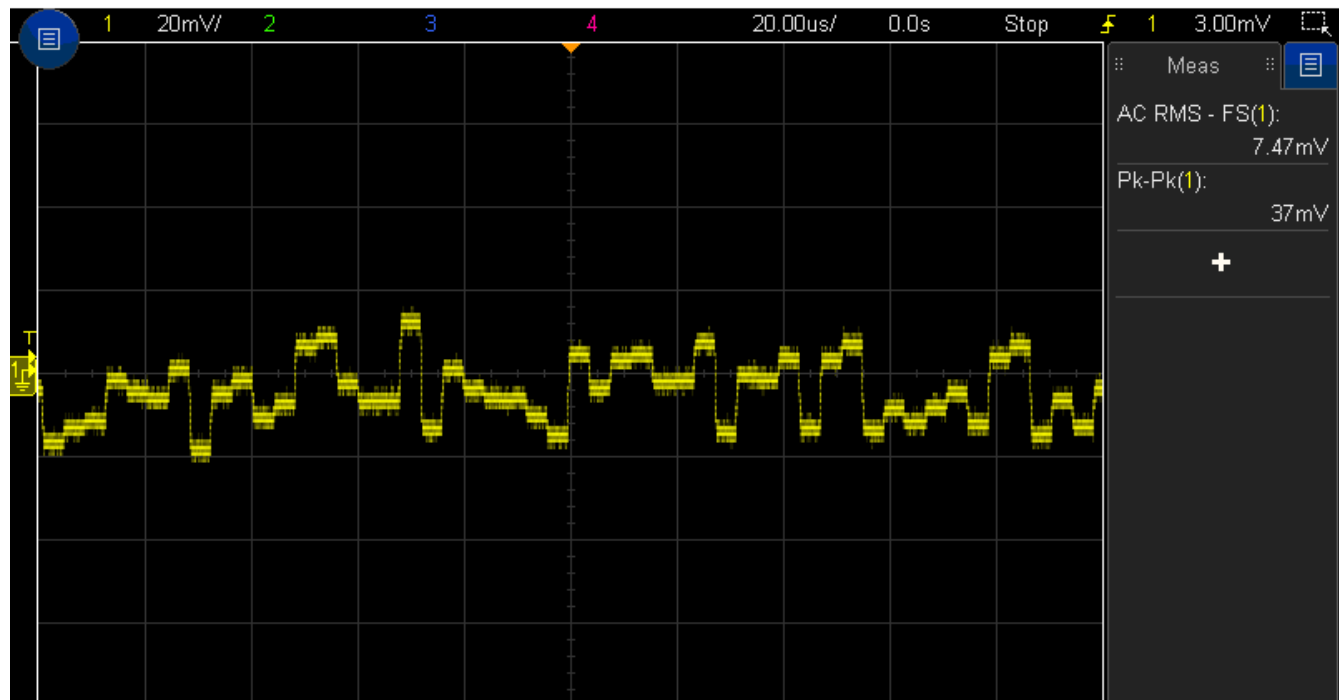
Figure 4-1. A1 Variant Noise Floor With RMS and P2P Values
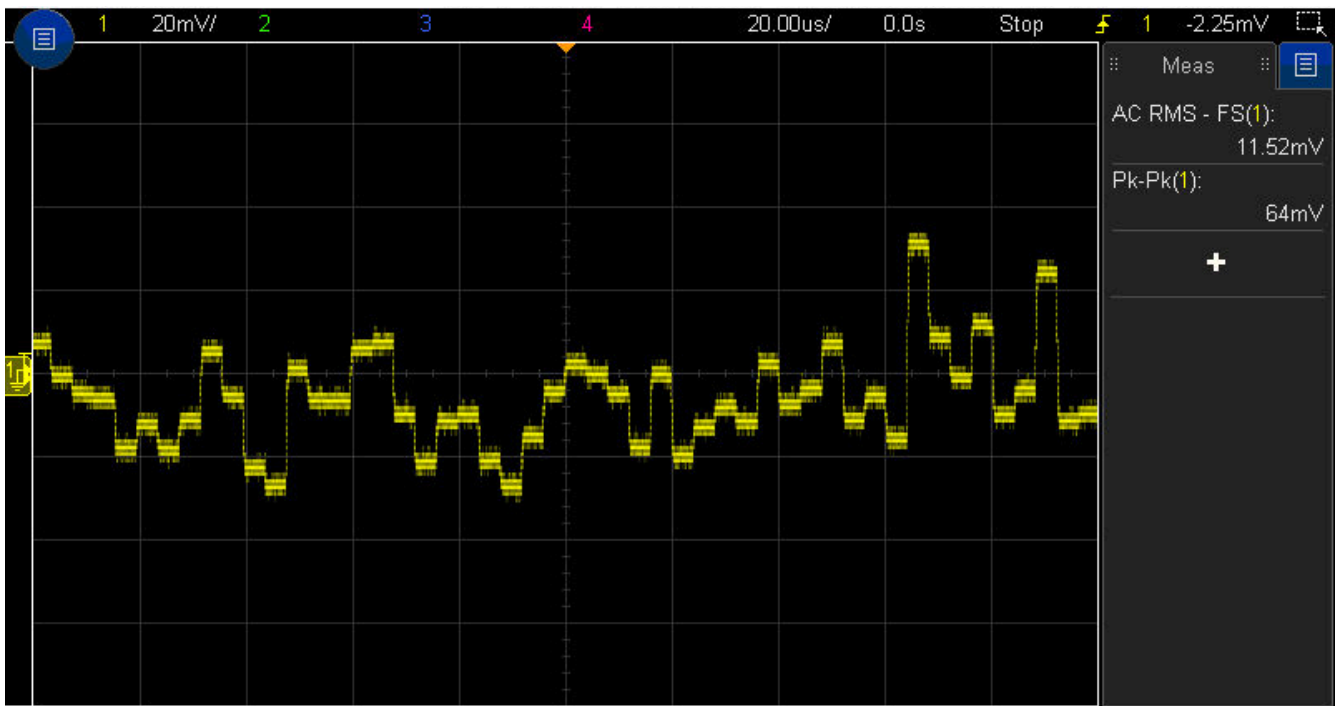
Figure 4-2. A2 Variant Noise Floor With RMS and P2P Values
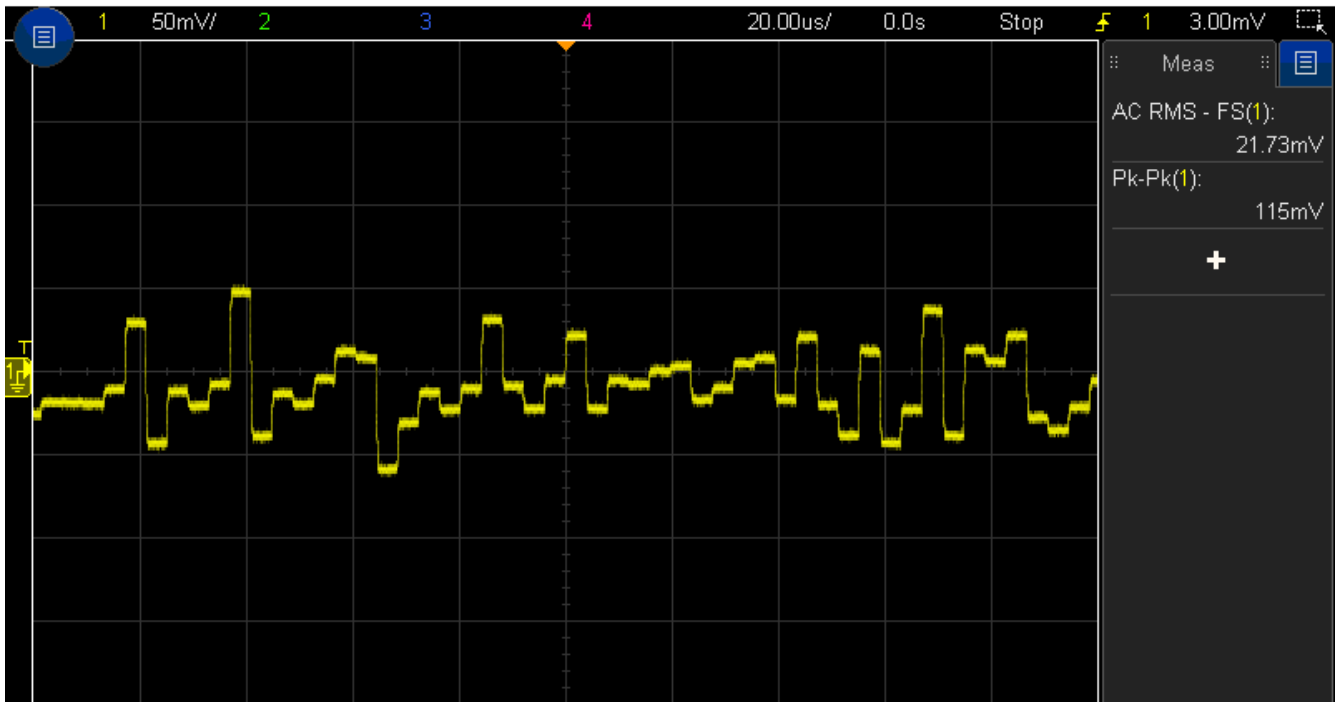
Figure 4-3. A3 Variant Noise Floor With RMS and P2P Values
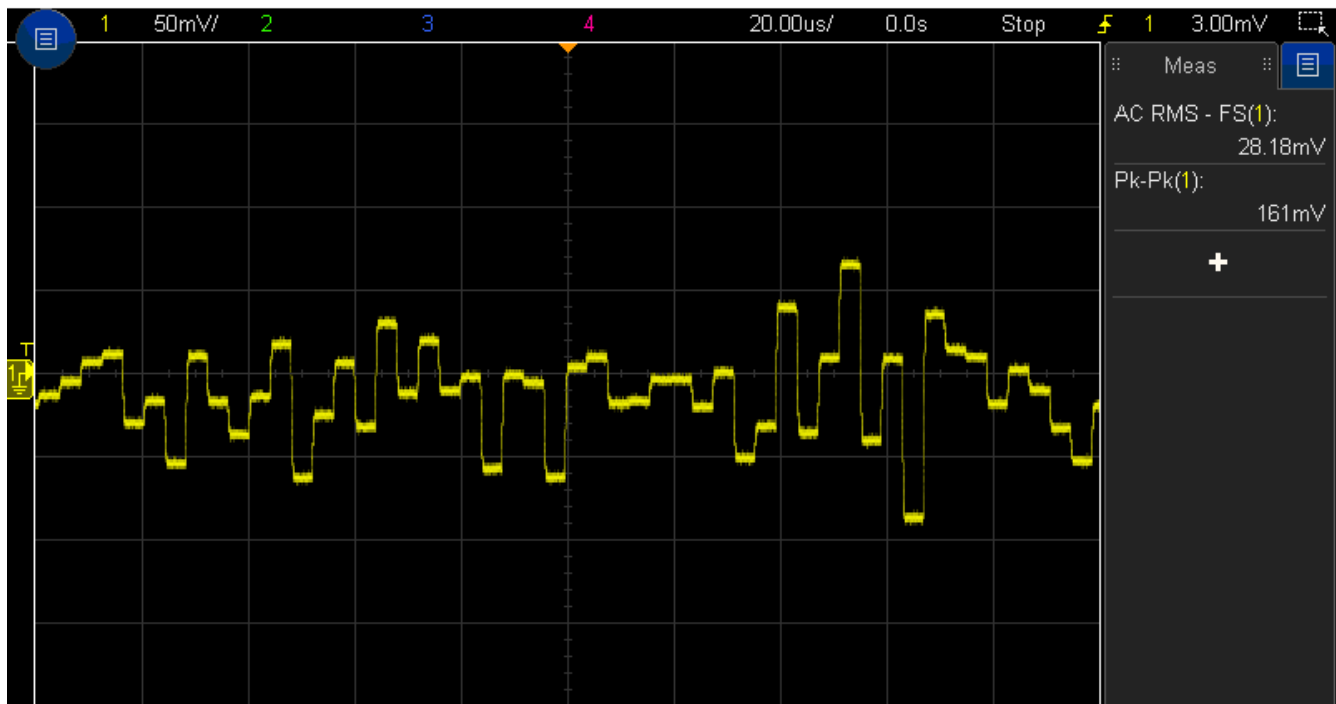
Figure 4-4. A4 Variant Noise Floor With RMS and P2P Values

A common technique used to resolve small signals in the presence of noise is to increase overall Signal-to-Noise Ratio (SNR) by limiting the Noise Equivalent Bandwidth (NEBW) using a low-pass filter on the output of the device. When sized properly, a simple low-pass filter attenuates overall noise contributions from the 250-kHz signature of the sampling integrator. This implementation attenuates contributions from the 250-kHz signature of the sampling integrator, as well as reduces noise spectrum contributions from the portion of bandwidth attenuated by the new cutoff frequency. Figure 4-5 through Figure 4-8 show the improvement of the noise floor of the A2 variant for various cutoff frequencies. Note from A2 Output with Low-Pass Filter, Cutoff Frequency = 80 kHz that even a low-pass filter set at the bandwidth of the part provides improvement. While this filter does not reduce noise contributions, it attenuates steps from the 250-kHz signature on the output without degrading output fidelity.
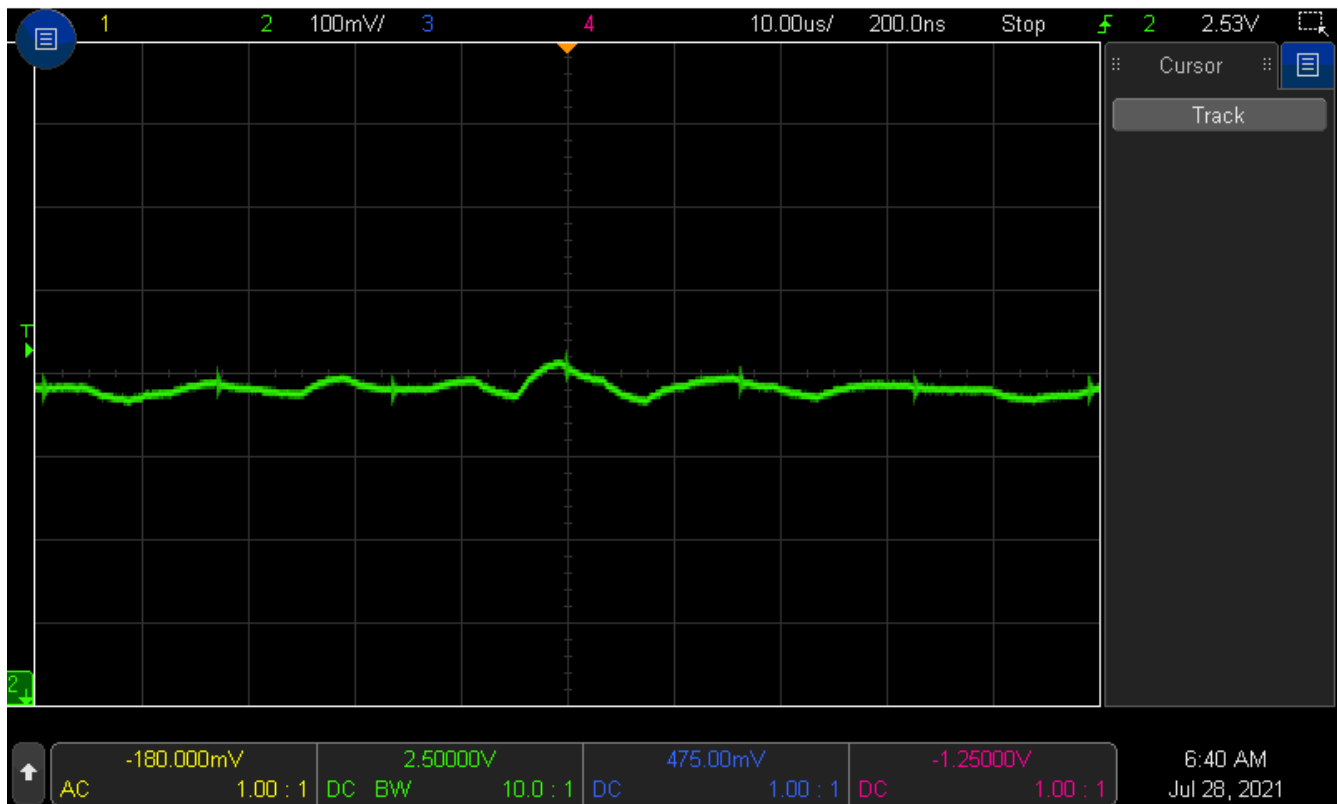
Figure 4-5. A2 Output With Low-Pass Filter, Cutoff Frequency = 100 kHz
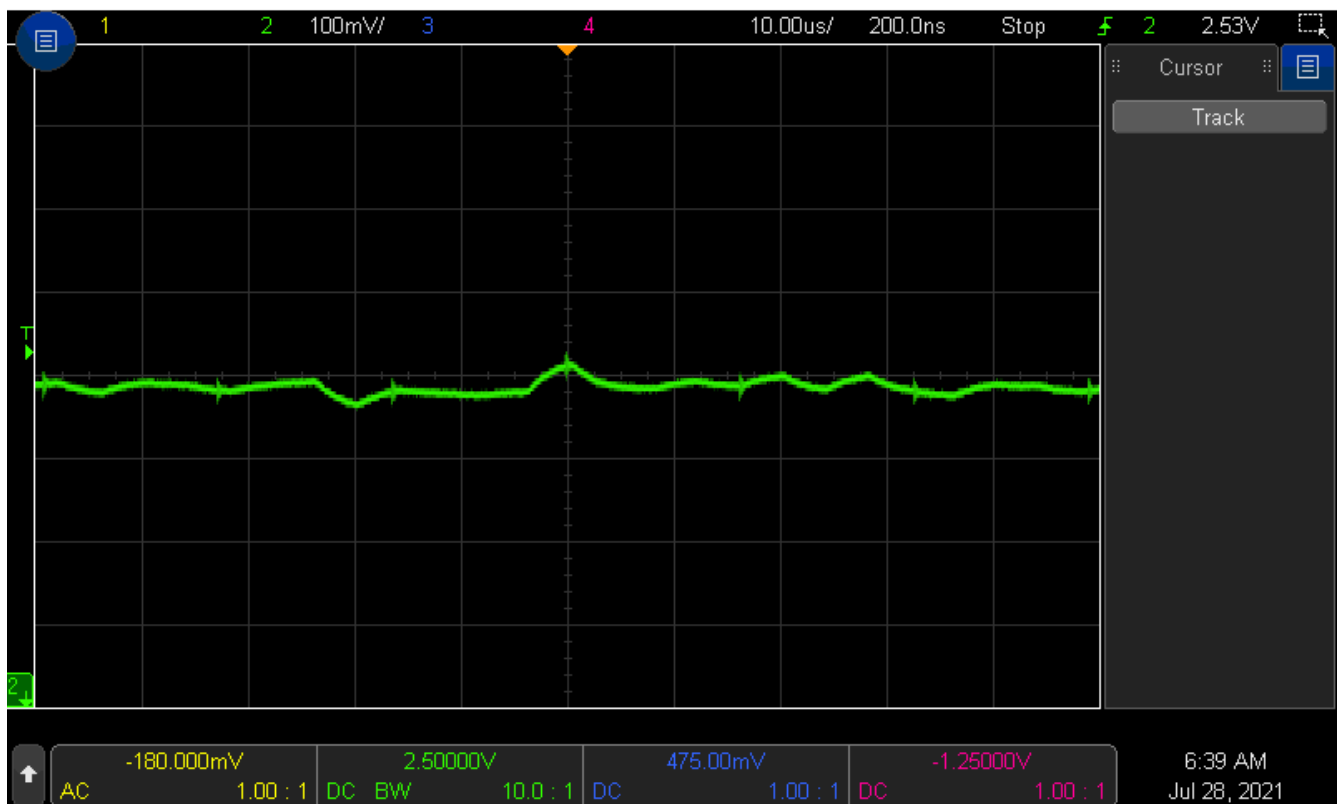
Figure 4-6. A2 Output With Low-Pass Filter, Cutoff Frequency = 80 kHz
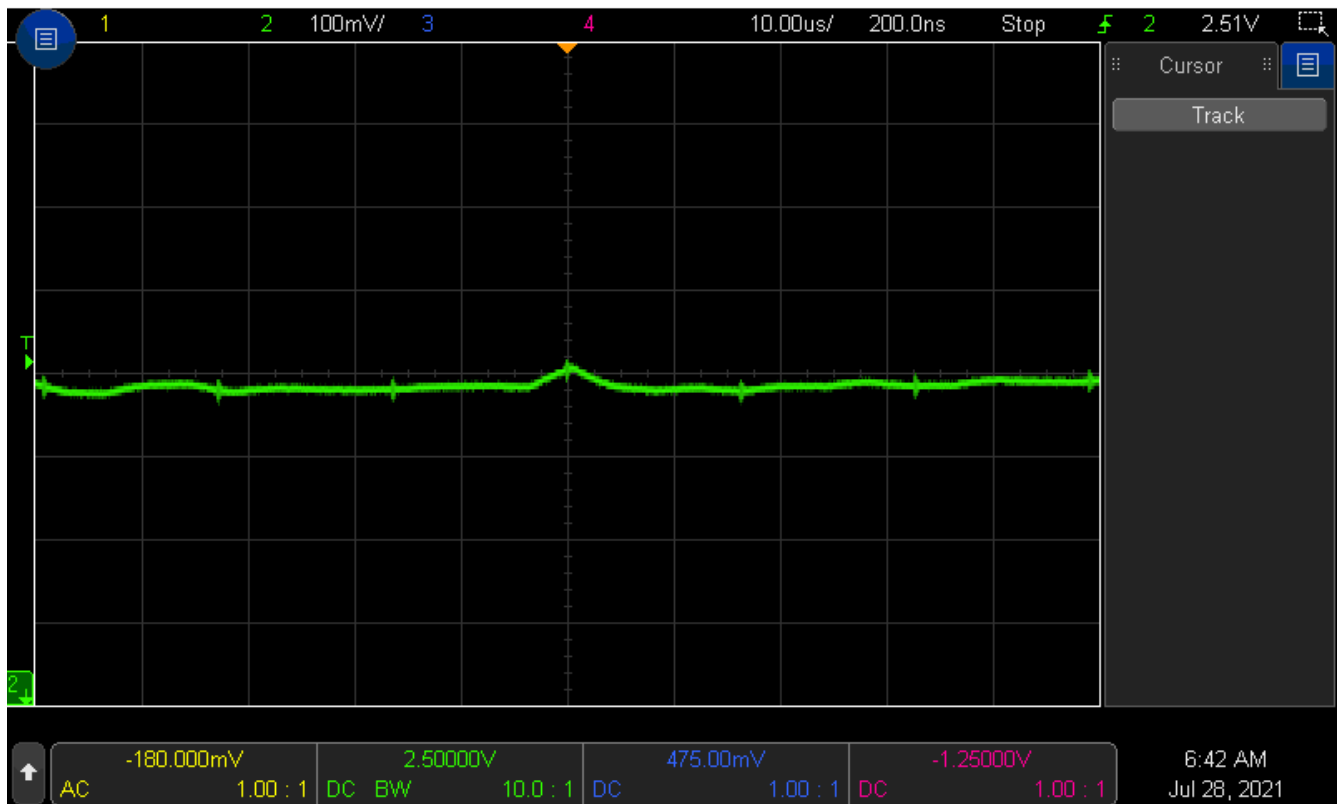
Figure 4-7. A2 Output With Low-Pass Filter, Cutoff Frequency = 40 kHz
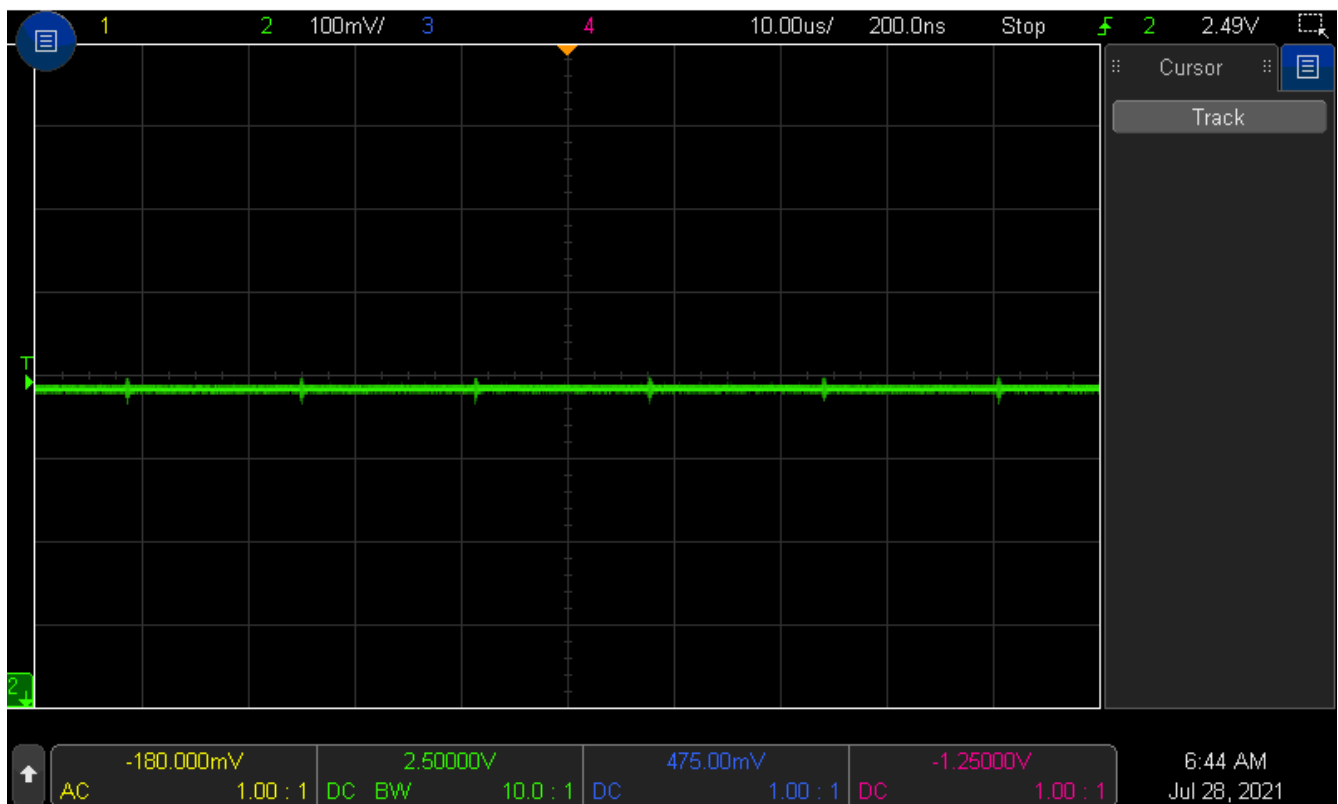
Figure 4-8. A2 Output With Low-Pass Filter, Cutoff Frequency = 500 Hz

5 External Fields

When working with Hall sensors, external magnetic sources can influence the measurement for any device that does not have any additional circuitry for removing external fields, such as the TMCS1100 and TMCS1101. The Hall sensors present in such devices are unable to differentiate when it comes to a sensed magnetic field. Utilizing the magnetic coupling factor found in the data sheet, the sensors inside the package amplify the sensed field, and therefore the presence of any unwanted fields is manifested as an error on the output of the device.

With a quantifiable value of an external field, use Equation 6 to approximate the error produced internal to the TMCS110x from an external field. For a static field, this manifests as an offset in the measurement, while a dynamic or periodic field may look like a random signal coupled onto the output.

$$\% \, \text{Error}_{\text{externalB}-\text{field}} = \frac{B_{\text{external}}}{B_{\text{ideal, internal}}} \times 100 \, \% \tag{6}$$

where

$$B_{\text{ideal, internal}} = \text{Load} \;\; \text{Current} \times \text{Magnetic} \;\; \text{Coupling} \;\; \text{Factor} \tag{7}$$

Recognizing that unaccounted external magnetic fields may lead to measurement error, it is imperative to identify what might produce such fields. These fields are not limited to sources external to a board under analysis, but can also be due to various components and structures on the board, as well as externally coupled sources, including and not limited to the Earth's magnetic field.

## 5.1 Earth's Magnetic Field

One external magnetic source that is unavoidable in most operating settings is the Earth's magnetic field, which ranges in magnitude from 22 µT to 67 µT at the Earth's surface depending on location and orientation. This error source can be quite important to consider, especially if the end equipment using the Hall-effect sensor is expected to capture precision measurements, and is traveling to multiple locations. Earth's Magnetic Field Diagram provides a simplified illustration of how the flux lines emanate out of the Earth. In reality, these flux lines will be slightly distorted. On a grand scale this may be due to variation in the material makeup of the Earth, while on a smaller scale this might be due to the materials of the building or structure in which the measurement device is housed.
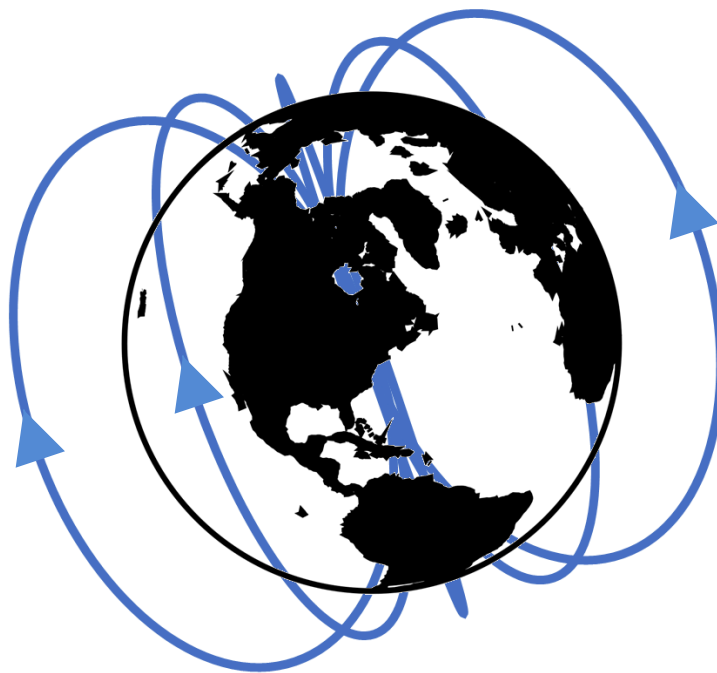
Figure 5-1. Earth's Magnetic Field Diagram

As Earth's magnetic field is a vector quantity, the impact in design is influenced not only by the magnitude of the field, but also by the orientation of the device, which is important to consider if precision measurements are needed inside an end equipment that does not remain stationary.

As an example, Local Observations of Earth's Magnetic Field on TMCS1100A2, V_{REF} = 2.5 V provides measurements that were captured for x, y, and z axes respectively for a TMCS1100EVM locally in the magnetics lab in Tucson, AZ, to show the potential skew in output as the device orientation changes. Note that yaw rotation resulted in no change to the output, which is expected: the orientation of the device against the **B** vector does not change for this rotation.

Table 5-1. Local Observations of Earth's Magnetic Field on TMCS1100A2, V_{REF} = 2.5 V

Orientation	Output Voltage, 0 deg (V)	Output Voltage, 90 deg (V)
Roll (X-axis)	2.486	2.500
Pitch (Y-axis)	2.489	2.492
Yaw (Z-axis)	2.504	2.504

As mentioned previously, however, this data is meant as an example only, and a similar test such as this may be required locally to quantify this impact for a given area, as the magnitude, as well as vector orientation, of the earth's field changes by location.

5.2 Conduction Paths

Another somewhat unavoidable source of magnetic fields is any current-carrying wire, which includes all surrounding PCB traces and wires as well as the input lines into the Hall-sensing device. Consequently, more attention must be devoted to layout than that of a conventional current shunt monitor. The amount of field a current-carrying wire imposes upon the Hall-sensing element of the device can be determined mathematically via Ampere's Law, given in Equation 8.

$$\overrightarrow{B} = \frac{\mu_0 \times I}{2\pi r} \tag{8}$$

This equation requires the magnitude of the current carried in the wire under analysis, as well as the orthogonal distance of the wire to the sensor located in the TMCS110x device. This equation allows for the approximation of the external field generated by wires or traces, and may be useful for creating design rules for PCB layout that ensure that traces remain a certain distance away from the sensor to ensure optimization of the generated field.

For example, consider a trace on a PCB located 15 mm from a TMCS1101. For the TMCS110x family, the location of the sensor may be approximated as the center of the package. Examining the data sheet for D0008B package information, the worst case distance to the outer footprint of the package is 2.9 mm, taking the pins of the device into account. This is visualized in Example - Distance From Trace to Sensor.
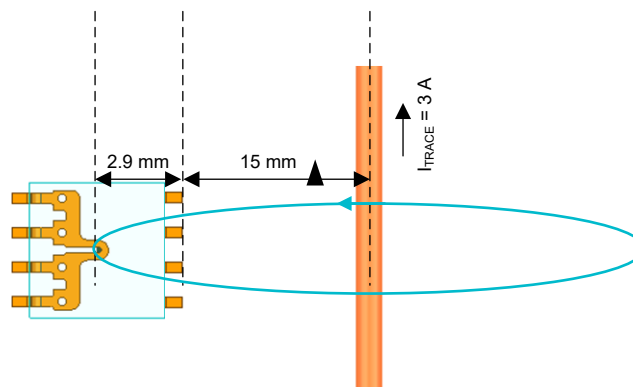
**Figure 5-2. Example - Distance From Trace to Sensor**

Equation 9 and Equation 10 show that the contribution from this trace at this distance is potentially 33.5 μT in the positive z direction at the point of the sensor, or a –30.45 mA offset current referred to the input. Also, note that this calculation needs to be performed for each trace in proximity to the TMCS110x, as each current-carrying

conductor exhibits an influence on the sensor. Right hand rule should also be taken into account, because the directionality of current flow also dictates the polarity of the contributed field.

$$\vec{B} = \frac{\mu_0 \times I}{2\pi r} = \frac{4\pi \times 10^{-7} \times 3\,A}{2\pi(15\,mm + 2.9\,mm)} = 33.5\,\mu T \quad \left(\text{positive } Z \text{ direction}\right) \tag{9}$$

$$I_{OFFSET} = \frac{\vec{B}}{\text{Magnetic Coupling Factor}} = \frac{33.5\,\mu T}{1.1\frac{mT}{A}} = -30.45\,mA \tag{10}$$

While it is straightforward to isolate high current traces from the TMCS110x, a more challenging observation is that the input current approach external to the device also has the potential to contribute an external field. To examine the effects of this, a 3D printed structure was created to insert an insulated wire pair at fixed 10-mm intervals from the TMCS1100EVM. TMCS1101 Bifurcation Test Board shows the construction of the 3D printed housing and test set up. Data was captured via this setup for a typical device, and TMCS1101 Bifurcation Test Results shows the typical effects of the proximity of these wires across a range from 10 mm to 150 mm from the input pins of the device.
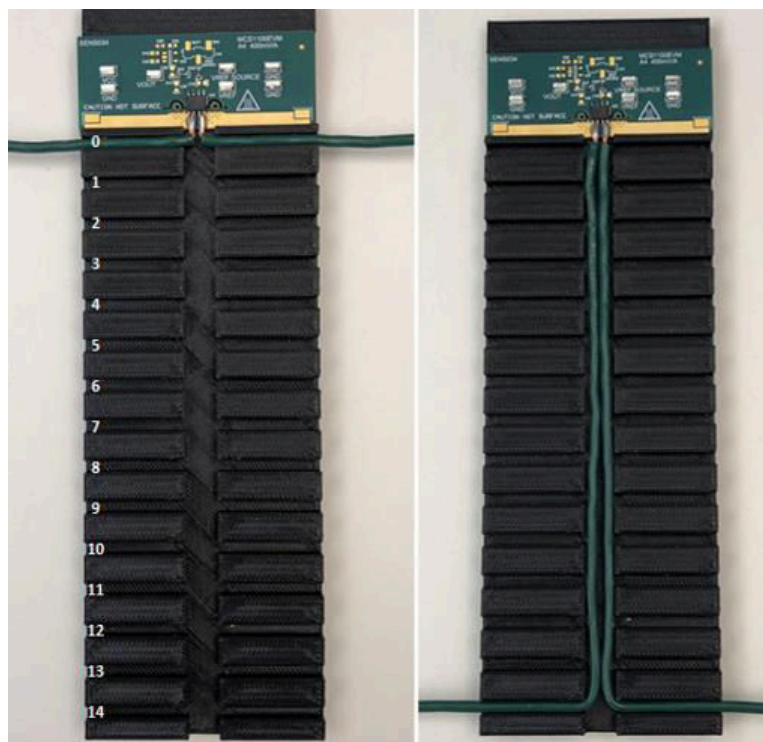

**Figure 5-3. TMCS1101 Bifurcation Test Board**
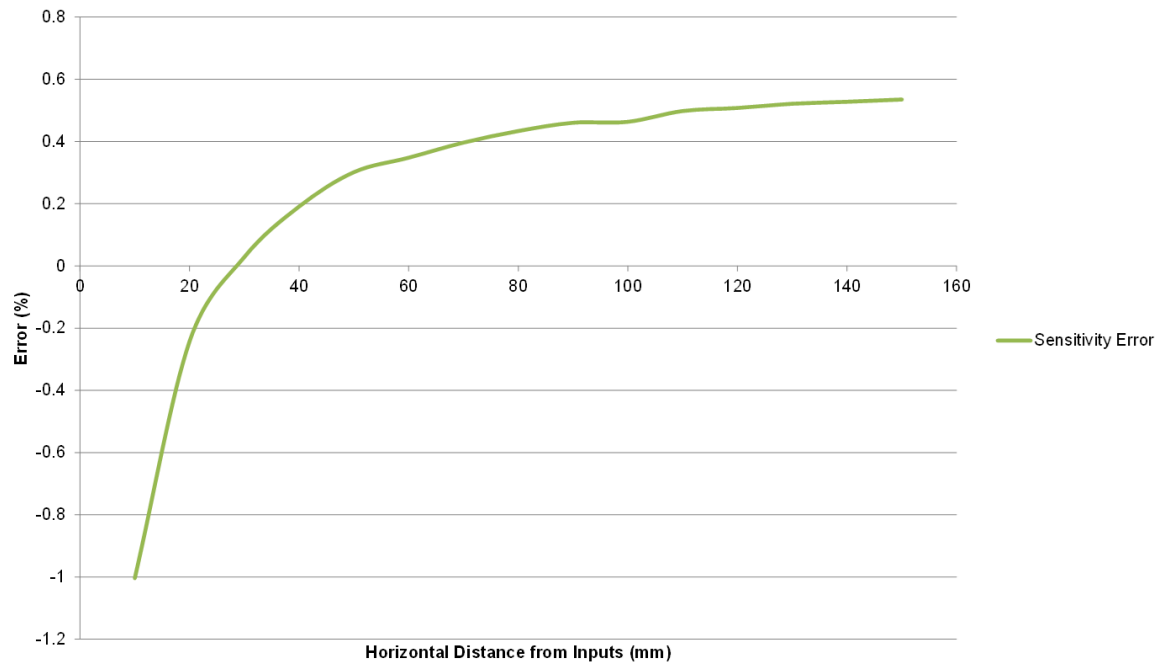
Figure 5-4. TMCS1101 Bifurcation Test Results

Observation indicates that the external field shifts the error of the TMCS1101 as the traces approach the device, and minimizes their contribution as the traces move further away from the device. Also note that from these observations the recommended angle of approach for the TMCS110x family is directly into the pins of the device for best performance. This is demonstrated on the TMCS1100EVM and TMCS1101EVM. Deviation away from a head-on approach may require layout calibration for optimized results. See the Calibration section for additional details.

5.3 Additional Magnetic Components

In addition to currents traversing a PCB, some magnetic components may also provide external field contributions that must be accounted for to ensure they do not impact, or provide minimal impact to the sensor.

The most common magnetic components observed on PCBs are inductors and transformers. These elements have the potential to radiate to nearby components, although the main component of their fields is typically found in the core material. As these devices are typically powered in a somewhat constant fashion, the easiest way to mitigate their effects is to ensure they are placed at some distance on the PCB from the sensor.

Also consider magnetic relays as a potential source of magnetic emanation, because these devices may also radiate magnetic fields when they are powered on or off, based on their configuration. A straightforward way to circumvent this is to use strategic design options in their place, such as latching relays. These devices, while still magnetic in nature, latch into place and do not hold a magnetic field through current in a coil. The coil quickly engages, and flips a switch internal to the device. This helps to mitigate the potential stray field, because it is only during switching that a magnetic field is produced.

Finally, although obvious, permanent magnets continue to find their way into electronics at an increasing pace. In static applications, such as alignment magnets for true wireless earbud chargers, or the locking mechanism of a case, as well as in more dynamic configurations, such as the rotor-mounted pole magnet used for motor commutation, permanent magnets are being implemented at a greater rate with each new iteration of technology. These devices will also emit constant, in some cases, extremely powerful magnetic fields that must be taken into account when determining the ideal layout for a Hall-effect sensor.

6 External Field Mitigation

Because external ambient fields are always present to some magnitude in an operating setting, knowing how to compensate for them or mitigate their influence is necessary for ensuring good measurement accuracy. Aside from placing distance between the magnetic sources and the TMCS110x device, there are a few general methods that may be applied to minimize the impact of external fields. As mentioned in Section 5, proper spacing and isolation on the board itself is a straightforward method here. Another method is to provide shielding to effectively divert the field away from the Hall sensor. Finally, calibration in post processing may be another potential option to investigate.

6.1 Shielding

Shielding utilizes the property of reluctance, which for magnetic fields is analogous to resistance for current. Magnetic fields route through the path of least reluctance. Inversely related to reluctance is permeability. Materials with high permeability have low reluctance and therefore are highly desirable for shielding, which actually serves to divert the magnetic field away from the Hall sensor. The material chosen, based on its permeability, must be of a certain thickness to ensure that it is capable of diverting the totality of the field away from the part, because shielding material is also capable of saturation. If the shielding material saturates, excess magnetic flux continues to pass through the material and exert influence on the sensors.

To better visualize how shielding works, an example of a shield and concentrator are provided in Figure 6-1 and Figure 6-2. In both images, there is a uniform field of several µT directed through the examined volume along the Z-axis.

The first figure shows the cross-sectional area of the XZ plane, and that the shell of the shield diverts a majority of the field, with the space internal to the sphere at much lower magnitudes of field strength than that diverted by the shield.

The second figure inserts a conical concentrator structure into the same field above and below the device. Here, the XZ cross section is also examined. The upper cone structure channels the majority of the field entering the base towards the cone tip where it then exits and passes into the tip of the bottom cone and continues to move downward. Note that such a structure is the dual to the shield of the first figure, and is not recommended as a shielding geometry. This also means that any wires or flux carrying components placed over the device may influence measurements, including while debugging, so ensure these types of devices are kept in check from the sensor.
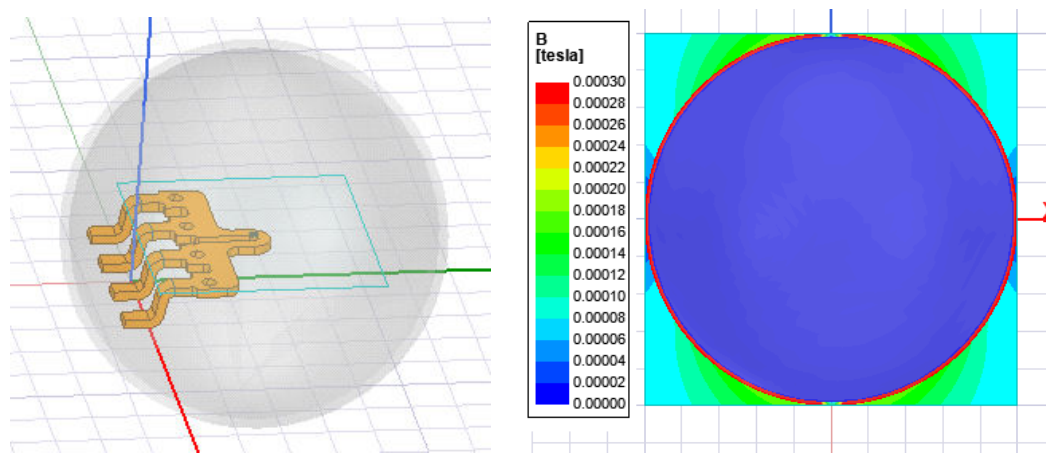

**Figure 6-1. Spherical Shield Layout and Simulated Field Deflection (Side View)**
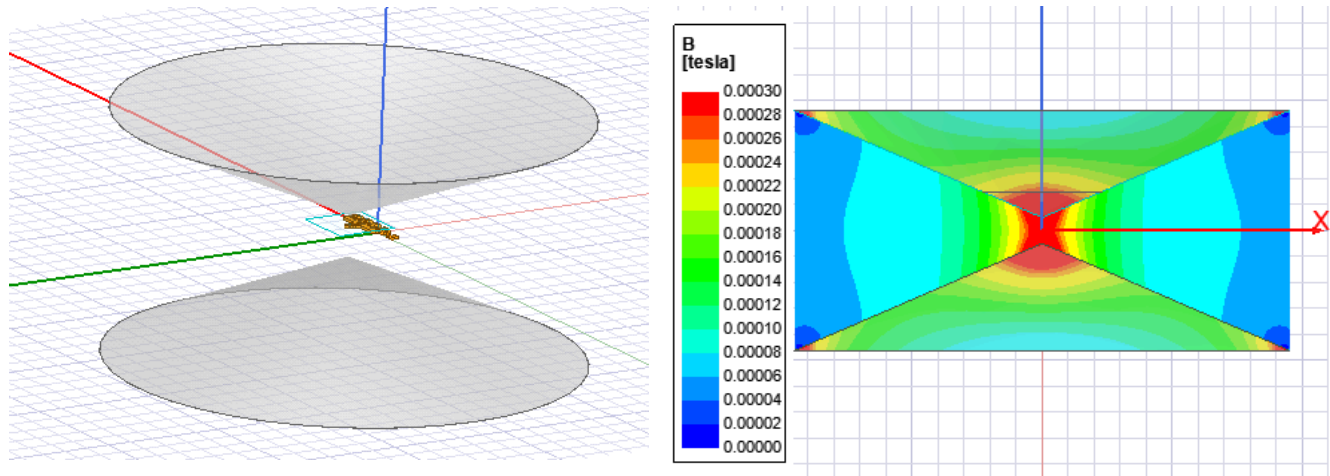
Figure 6-2. Conical Concentrator Layout and Simulated Field Concentration (Side View)

Note that for the illustration, a perfect spheroid is likely unattainable when manufacturing or choosing shield shapes, nor is completely enclosing the device as shown in the simulation. This image is meant as a concept for visualization, and certain geometries may work more effectively than others in a given system.

In summary, if shielding is chosen as a method for field mitigation, ensure that the correct material is chosen, that it is shaped appropriately, and it is sized to ensure proper field diversion.

6.2 Calibration

The term calibration must be used cautiously here, as technically three calibration options exist that can be performed with the TMCS110x: a one-time layout sensitivity calibration, and then an "up to two step" process: a one-point offset device calibration, and a device level sensitivity calibration if additional accuracy is desired beyond the one point calibration routine. Note that the latter of these options is device specific, requiring unique values to be programmed in firmware, and thus adding complexity in applications requiring scalability.

The first option mentioned is a calibration based on layout and entry angle of the current into the TMCS110x device. A good example of the errors under consideration here are those discussed in Conduction Paths. The entry angle of the current, as well as other potential factors, may shift the sensitivity due to their proximity and contributions to the TMCS110x. To perform this calibration, two known currents are applied to the TMCS110x, and the corresponding outputs measured. From these points, the true sensitivity of the device is calculated via point-slope form, that is, sensitivity is calculated as $\Delta V_{OUT}/\Delta I_{IN}$. Once this slope is determined, it is held in logic and the output may then be data corrected in logic via this coefficient in place of the ideal device value from the data sheet. Once this calibration to the layout is performed, the expected variation is then limited from device to device by the maximum sensitivity error in the data sheet.

A second calibration step for additional accuracy is to then eliminate DC offsets potentially present in the system. This is typically performed once the device is in place (in terms of application, not layout), and will remain stationary, as the Earth's magnetic field or any other DC fields may change if the orientation changes. This calibration is performed via a zero current condition placed at the inputs, and measuring the corresponding output. In an ideal sense, under this condition, the output voltage is the reference voltage of the device. The deviation between this expected ideal and the actual output being measured is the DC offset under discussion. The expected output for each device is shown in TMCS1101 Data Sheet: Linear Operating Region and is corrected to this measured value in logic. Note, as mentioned before, this type of calibration is device *and* orientation specific and should be done for each device when the board is its expected use location.

The final calibration option may be implemented if the first calibration does not provide enough error correction, and additional accuracy is required. This calibration is simply repetition of the board level calibration, but is performed for each specific device, rather than a blanket coefficient to the layout itself. This eliminates the device variation in sensitivity, and removes the sensitivity at a given operation point. Note that unaccounted for external fields, or outside factors such as temperature drift may still introduce additional error here.

7 Summary

This document examined several facets of device operation and specification related to the TMCS110x device sensitivity, and discussed several options for best practices in layout and design. However, other factors not related to the sensitivity of the device should also be taken into consideration, such as common-mode rejection ratio (CMRR), power supply rejection ratio (PSRR), and offset.

In addition to these practices, take thermal considerations into consideration when designing with the TMCS11xx product family. Additional information on thermal design is discussed in *Thermal Implementation Guide for In-Package Magnetic Current Sensors* application note.

IMPORTANT NOTICE AND DISCLAIMER